

1 **Evaluation of NanoLuc, RedLuc and Luc2 as bioluminescent reporters in a cutaneous**
2 **leishmaniasis model**

3 Victor S. Agostino ^a; Cristiana M. Trinconi ^a; Mariana K. Galuppo ^a; Helen Price ^b; Silvia R. B.
4 Uliana ^{a,*}

5 ^a Department of Parasitology, Biomedical Sciences Institute, University of Sao Paulo, Sao
6 Paulo, CEP 05508-000; Brazil;

7 ^b Centre for Applied Entomology and Parasitology, School of Life Sciences, Keele University,
8 Newcastle-under-Lyme, Staffordshire, ST5 5BG, United Kingdom.

9

10 *Corresponding author: E-mail address: srbulian@icb.usp.br (S. Uliana).

11
12
13
14
15
16
17
18
19
20
21
22
23
24
25
26
27
28
29
30

Abstract

New drugs for the treatment of human leishmaniasis are urgently needed, considering the limitations of current available options. However, pre-clinical evaluation of drug candidates for leishmaniasis is challenging. The use of luciferase-expressing parasites for parasite load detection is a potentially powerful tool to accelerate the drug discovery process. We have previously described the use of *Leishmania amazonensis* mutants expressing firefly luciferase (Luc2) for drug testing. Here, we describe three new mutant *L. amazonensis* lines that express different variants of luciferases: NanoLuc, NanoLuc-PEST and RedLuc. These mutants were evaluated in drug screening protocols. NanoLuc-parasites, in spite of high bioluminescence intensity *in vitro*, were shown to be inadequate in discriminating between live and dead parasites. Bioluminescence detection from intracellular amastigotes expressing NanoLuc-PEST, RedLuc or Luc2 proved more reliable than microscopy to determine parasite killing. Increased sensitivity was observed *in vivo* with RedLuc-expressing parasites as compared to NanoLuc-expressing *L. amazonensis*. Our data indicates that NanoLuc is not suitable for *in vivo* parasite burden determination. Additionally, RedLuc and the conventional luciferase Luc2 demonstrated equivalent sensitivity in an *in vivo* model of cutaneous leishmaniasis.

Keywords: *Leishmania*; drug screening; bioluminescent reporters; bioimaging; NanoLuc; red-shifted luciferase.

31 **1. Introduction**

32 The leishmaniasis are a complex group of devastating diseases with a wide clinical
33 spectrum varying from self-healing tegumentary to fatal visceral forms. Over 20 species of
34 *Leishmania spp.* are pathogenic to humans leading to variable clinical manifestations
35 depending on the parasite species and host immunological response. Within the tegumentary
36 form, the disease can be further classified in cutaneous, mucocutaneous, diffuse and
37 disseminated leishmaniasis (Burza et al., 2018). *Leishmania (Leishmania) amazonensis* is
38 one of the most prevalent agents of human cutaneous leishmaniasis (CL) in the Amazon
39 region of Brazil. It is also the main etiological agent of diffuse cutaneous leishmaniasis (DCL)
40 in South America (Convit et al., 1993), a rare and aggressive form of disease characterized
41 by the appearance of multiple non-tender and non-ulcerating papules or nodules widespread
42 in the body. DCL is a chronic disease and is considered refractory to the current available anti-
43 *Leishmania* therapeutic arsenal (Zerpa et al., 2007).

44 The parasite can be transmitted by several species of female hematophagous
45 sandflies, most of them within the genus *Phlebotomus*, in the Old World, and *Lutzomyia*, in
46 the New World (Akhoundi et al., 2016). Leishmaniasis are distributed worldwide and endemic
47 in over 90 countries or territories. According to the World Health Organization, the annual
48 incidence of the disease is approximately 1 million new cases (Bern, Desjeux, Cano, & Alvar,
49 2012; WHO, 2015).

50 The treatment of leishmaniasis is limited to a few drugs and most of them have been
51 in use for a long time without significant upgrading (Uliana et al., 2017). The therapeutic
52 arsenal currently available includes pentavalent antimonials, amphotericin B, pentamidine,
53 miltefosine and paromomycin. Miltefosine is the only drug which is administered orally (Sundar
54 and Olliaro, 2007), whereas all the others must necessarily be administered parenterally. All
55 those drugs may induce serious side effects, ranging from nephro-hepatotoxicity to
56 teratogenicity (Sundar and Singh, 2017). The toxicity is even more pronounced in
57 malnourished patients, a common occurrence with advanced visceral leishmaniasis.
58 Moreover, loss of efficacy of pentavalent antimonials and miltefosine has been reported

59 (Ponte-Sucre et al., 2017). Thus, the identification of new drugs for leishmaniasis treatment
60 with better efficacy and safety profiles is an urgent issue.

61 Preclinical drug development against leishmaniasis includes *in vitro* and *in vivo* tests.
62 *In vitro* tests are preferably performed against the intracellular amastigote stage and *in vivo*
63 tests employ animal models, mostly mice and hamsters. The use of reporter proteins
64 detectable in intact animals represented a great advance for the challenging demonstration of
65 drug efficacy of antileishmanial compounds in experimental models of the disease (Calvo-
66 Alvarez et al., 2018; Jaiswal et al., 2016; Rocha et al., 2013). Furthermore, the strategy
67 addresses the important ethical aspects of reducing the number of animals needed for each
68 experiment as well as refining the handling and information derived from each animal (two out
69 of the 3Rs advocated for ethical pre-clinical research. We have previously employed mutant
70 parasite lines expressing a modified firefly luciferase as an experimental tool for testing
71 candidate compounds *in vitro* and *in vivo* (Reimão et al., 2015, 2013; Trinconi et al., 2016).

72 Luciferases are a class of enzymes commonly found in nature in fireflies and in several
73 marine organisms, such as jellyfish or copepods, that generates light in the presence of a
74 specific substrate (Avci et al., 2018; Yan et al., 2019). Natural luciferases have been
75 genetically modified to improve their specific activity, through increased intensity of light
76 production, and/or altered wavelength to improve detection. Amongst many modified
77 luciferases already produced, three of these were chosen for the analysis described here:
78 RedLuc (RL), NanoLuc (NL) and its variation NanoLuc-PEST (NLP). NL and NLP were derived
79 from Oluc, a luciferase isolated from the deep-sea shrimp (*Oplophorus gracilirostris*) (Hall et
80 al., 2012). NL was shown to achieve greater efficiency than the parent protein in the presence
81 of furimazine, its appropriate substrate, modified from coelenterazine (Hall et al. 2012).
82 Furthermore, NL's intracellular half-life of 6 hours leads to intracellular accumulation of the
83 enzyme, which also potentiates light emission. NLP was obtained by inserting a PEST motif
84 (García-Alai et al., 2006; Rechsteiner and Rogers, 1996) into the C-terminus region of the
85 protein, resulting in a shorter intracellular half-life of about 20 minutes. RedLuc, a red-shifted
86 luciferase, is a firefly (*Luciola cruciata*) luciferase gene modified by the substitution of an

87 isoleucine by a valine in the position 48 (p.I48V), which modifies the substrate (luciferin)
88 cleavage, resulting in the production of light with a wavelength above 600 nm (Branchini et al.,
89 2005a). Long wavelength light can penetrate more easily in tissue barriers, which could
90 potentially enhance the sensitivity detection of lower parasite burdens.

91 Here, we described the application of these modified luciferases (NL, NLP and RL) *in*
92 *vitro* and in an *in vivo* model of cutaneous leishmaniasis.

93

94 **2. Materials and Methods**

95 *2.1 Parasites*

96 Wild-type *Leishmania amazonensis* (MHOM/BR/1973/M2269) was cultivated at 25°C
97 in 199 culture medium (Sigma-Aldrich, St. Louis, MO, USA), complemented with HEPES 40
98 mM, pH 7.4, adenine 0.1 mM, hemin 0.005% and supplemented with heat-inactivated bovine
99 foetal serum 10% (Gibco®), and penicillin/streptomycin 100µg/ml. A mutant line of *L.*
100 *amazonensis* expressing Luc2, obtained as described (Reimão et al., 2015), was grown in
101 media supplemented with 32 µg/ml hygromycin. Mutant lines obtained in this work were
102 cultivated in media containing 32 µg/ml G418. Parasites were subcultured weekly.

103

104 *2.2. Generation of L. amazonensis line expressing the modified luciferases*

105 NL, NLP and RL constructs were obtained by cloning NanoLuc (616 bb), NanoLuc-
106 PEST (639 bp) and RedLuc (1647 bp) ORFs into the pSSU-Neo plasmid, which contains
107 complementary sequences to the *Leishmania* small subunit ribosomal DNA and a neomycin
108 resistance encoding gene (Berry et al., 2018). Upon transfection, the linearized plasmid was
109 expected to integrate into the parasite genome.

110 Promastigotes were transfected as previously described by Coburn et al.(1991) using
111 5 µg of linearized insert. After 24 hours, the selection drug (G418) was added to a
112 concentration of 32 µg/ml. Cultures were plated on semi-solid M199 medium supplemented
113 with 1.2 µg/mL biopterin, 1% agar, 2% urine and 32 µg/mL G418 for clone selection. Isolated
114 clones were randomly selected and expanded. Integration into the SSU rDNA was confirmed

115 through PCR amplification with primers complementary to sequences inside and outside the
116 transfected cassette. Primers S1 (5'-GATCTGGTTGATTCTGCCAG-3') and S4 (5'-
117 GATCCAGCTGCAGGTTCCACC-3') anneal to the SSU rDNA sequence (Uliana et al., 1991)
118 flanking the insertion sites, and primers NanoLuc-REV (5' TACCAGTGTGCCATAGTGCA 3'),
119 RedLuc-REV (5' ACGATGGTCTTGATGGTGGT 3') and Neo-FOR (5'
120 TATCGCCTTCTTGACGAGTTCT 3') are complementary to the cassette.

121

122 2.3. *Bioluminescence detection assay*

123 Logarithmic phase promastigotes were washed and suspended in PBS to a final
124 density of 10^6 promastigotes/mL. Parasites were serially diluted in final volumes of 100 μ L and
125 incubated in lysis buffer containing either furimazine (NanoGlo Assay System, Promega), for
126 mutants expressing NL and NLP, or luciferin (One-Glo luciferase Assay System, Promega),
127 for mutants expressing RL and Luc2. Furimazine was added to the lysis buffer in a 1:200 ratio
128 and luciferin was added in a 1:5 ratio. Bioluminescence was measured using a PolarStar
129 Omega luminometer (BMGLabTech).

130

131 2.4. *Susceptibility assays of intracellular amastigotes*

132 Bone marrow-derived macrophages (BMDM) were obtained as described (Reimão et
133 al., 2015) and plated in white 96-well plates (8×10^4 cells/well) or in 24-well plates (3×10^5
134 cells/well) with round glass coverslips applied to the bottom of the wells. After incubation for
135 24 hours at 37°C in a 5% CO₂ atmosphere, cells were infected with stationary phase
136 promastigotes (fourth day of culture) in a proportion of 20 parasites: 1 macrophage. After 4
137 hours incubation at 34°C, cultures were washed to remove the remaining free promastigotes.
138 Fresh medium containing several concentrations of miltefosine (Sigma-Aldrich), varying from
139 1 to 30 μ M, was added and the plates were incubated for 96 hours at 34°C. The supernatant
140 was discarded, and luciferase substrates were added to the 96-well plate as described in the
141 section 2.3. After homogenization, light production was detected in a PolarStar Omega
142 luminometer (BMGLabTech). Parasite survival in treated samples was determined based on

143 the ratio of treated/untreated cells. Macrophages cultivated in round coverslips were fixed with
144 50% methanol in PBS and stained with the Romanowsky type Instant Prov kit (Newprov,
145 Pinhais, PR, Brazil). The ratio of infected cells was calculated by counting 100 macrophages
146 per replicate. Half maximal inhibitory concentration (IC_{50}) was determined from
147 bioluminescence and microscopy assays by sigmoidal regression of the dose-response
148 curves using GraphPad Prism 8 software (CA, USA). Experiments were performed in triplicate
149 and repeated at least three times.

150

151 *2.5. Mice infection and parasite quantification*

152 Animal experiments were approved by the Ethics Committee for Animal
153 Experimentation (Protocol 178/2012) in agreement with the guidelines of the Sociedade
154 Brasileira de Ciência de Animais de Laboratório (SBCAL) and of the Conselho Nacional de
155 Controle da Experimentação Animal (CONCEA).

156 Female BALB/c mice (30 to 60 days-old) were inoculated subcutaneously with 10^6
157 stationary-phase promastigotes of La-NL, La-RL or La-Luc2 in the left hind footpad. Lesion
158 development was followed up weekly. Retrieval and purification of amastigotes from lesions
159 was done as described previously (Uliana et al., 1999). Quantification of amastigotes
160 recovered from lesions was performed by limiting dilution (Lima et al., 1997). Determination of
161 parasite burden was calculated using the formula $LDAU = GM \times RF$ (Calvo-Álvarez et al.,
162 2015), in which LDAU is the parasite burden indicated in limiting dilution assay units, GM is
163 the geometric mean of titer from the replicates and RF is the reciprocal fraction of the
164 homogenized lesion added to the first well. In this formula, titter is the last dilution where live
165 parasites were observed.

166 Bioluminescence quantification in live animals was performed as described (Reimão
167 et al., 2013). Imaging was performed after intraperitoneal administration of 75 mg/kg luciferin
168 (VivoGlo™, Promega) or 1:40 diluted furimazine (NanoGlo™, Promega) in sterile PBS and in
169 100 μ l final volume. Animals were anesthetized under a 2.5% isoflurane atmosphere and
170 transferred to the imaging chamber, where they were kept in a 1.5% isoflurane atmosphere

171 during imaging. Images were acquired 15 minutes after substrate administration using an IVIS
172 Spectrum (Caliper Life Sciences) with 2 minutes exposure time. Bioluminescence readings for
173 the whole animal were obtained. A region of interest (ROI) was defined as a region
174 encompassing an infected footpad. The same ROI (shape and size) was used to quantify
175 measured light units in all animals studied. Average radiance (photons/second/square
176 centimetre/steradian) was quantified by Living Image 4.3.1 (Caliper Life Sciences),
177 representing total photon emission from a ROI. A bioluminescence background was initially
178 obtained using the same ROI in an uninfected mouse. Alternatively, background was
179 measured using the ROI positioned at the contralateral uninfected footpad. The background
180 value was subtracted from all infected footpad readings. Pseudocolor imaging was generated
181 based on the photon signal to represent light intensity from the infected footpads, ranging from
182 red to blue meaning the most to the least intense.

183 For immediate quantification of light production by parasites inoculated in mice tissues,
184 10^5 stationary-phase promastigotes or amastigotes purified from lesions were inoculated in
185 the left hind footpad and animals were imaged one-hour post-injection.

186 Parasite burden of infected mice was also evaluated by *ex vivo* bioluminescence. For
187 these assays, the material recovered from lesions was suspended in 2 mL PBS and 20 μ L
188 from the total amastigote extract of each infected animal was incubated in the presence of the
189 respective substrate and submitted to bioluminescence quantification, as described above.

190

191 2.6. Statistical analysis

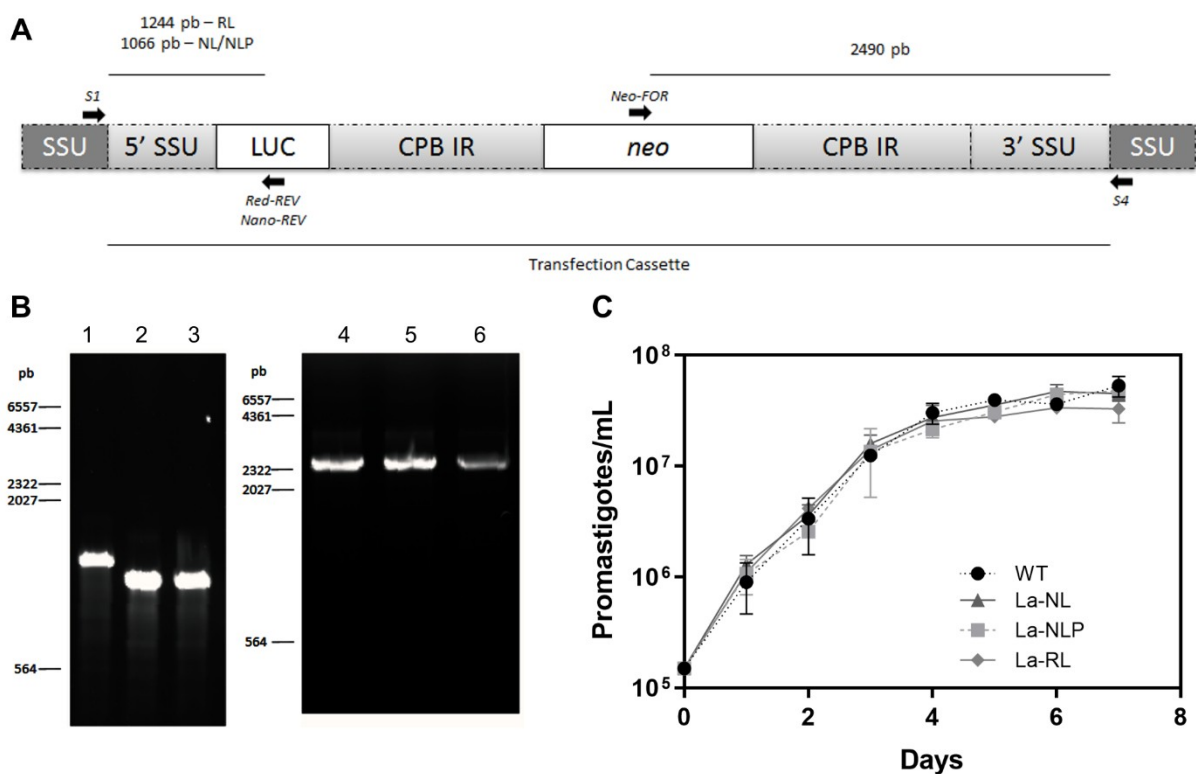
192 All statistical analyses were performed by GraphPad Prisma 8 (CA, USA), using
193 ANOVA *one-way* test and multiple comparisons Dunnett's test. *P* values ≤ 0.05 were
194 considered statistically significant.

195

196 3. Results and Discussion

197 3.1. Generation and phenotypic characterization of *L. amazonensis* mutants expressing 198 NanoLuc (NL), NanoLuc-PEST (NLP) and RedLuc (RL)

199 Constructs containing the modified luciferase genes were double digested with
 200 endonucleases *PacI* and *PmeI*, to linearize the cassette. Purified inserts (Fig. 1A) were
 201 transfected into wild-type (WT) *L. amazonensis* to generate mutants expressing NL (La-NL),
 202 NLP (La-NLP) and RL (La-RL). Integration into the small subunit rDNA (SSU) gene was
 203 assessed by PCR (Figure 1B). Primers for SSU sequences upstream and downstream to the
 204 expected integration region were designed and paired with primers corresponding to the
 205 luciferase gene or drug resistance marker (Fig. 1A). PCR products with the expected sizes
 206 confirmed the integration of the linearized DNA fragment in the expected *locus* (Fig. 1B).
 207 Clones were obtained and their growth curves were characterized. The growth of these
 208 transfected parasites was indistinguishable from the WT parasites (Fig. 1C), indicating that
 209 the integration of the cassette into the parasite genome did not impair cell growth.
 210



211

212 **Fig. 1. Generation of *L. amazonensis* transgenic lines expressing modified luciferases.**
 213 (A) Schematic representation of the linear cassette integrated into the SSU rDNA *locus*. SSU:
 214 small subunit rDNA; 5'/3' SSU: SSU homologous regions included in the cassette; LUC:
 215 coding sequence of modified luciferases; CPB IR: *L. mexicana* cysteine protease B intergenic
 216 region; *neo*: neomycin-phosphotransferase gene; arrows: primers used for PCR. (B)
 217 PCR products from La-RL (lanes 1 and 4), La-NL (lanes 2 and 5) and La-NLP (lanes 3 and 6)

218 genomic DNA with the pairs of primers S1/Red-REV (lane 1), S1/Nano-REV (lanes 2 and 3)
 219 and S4/Neo-FOR (lanes 4 to 6). (C) Growth curve of transfected and wild-type parasites.
 220 Results are the mean and standard deviation of a representative experiment of three
 221 independent experiments.
 222

223 The infectivity of *L. amazonensis* mutant lines *in vitro* was tested using BMDM. Cells
 224 were infected with stationary-phase promastigotes and maintained in culture for 48 hours. The
 225 percentage of infected macrophages and the number of amastigotes per macrophage were
 226 determined by optical microscopy and compared to infections with the WT parasite (Table 1).
 227 No significant differences were observed among the different mutant lines.
 228

229 Table 1. Evaluation of BMDM infection by WT and mutant *L. amazonensis* lines expressing
 230 modified luciferases.

	Infection (%)	Amastigotes/MØ
La-WT	56.6 ± 4,36	2.8 ± 0.3
La-NL	47.6 ± 4,04	2.0 ± 0.2
La-NLP	44.4 ± 3,78	1.9 ± 0.05
La-RL	43.1 ± 2,46	1.8 ± 0.1

231

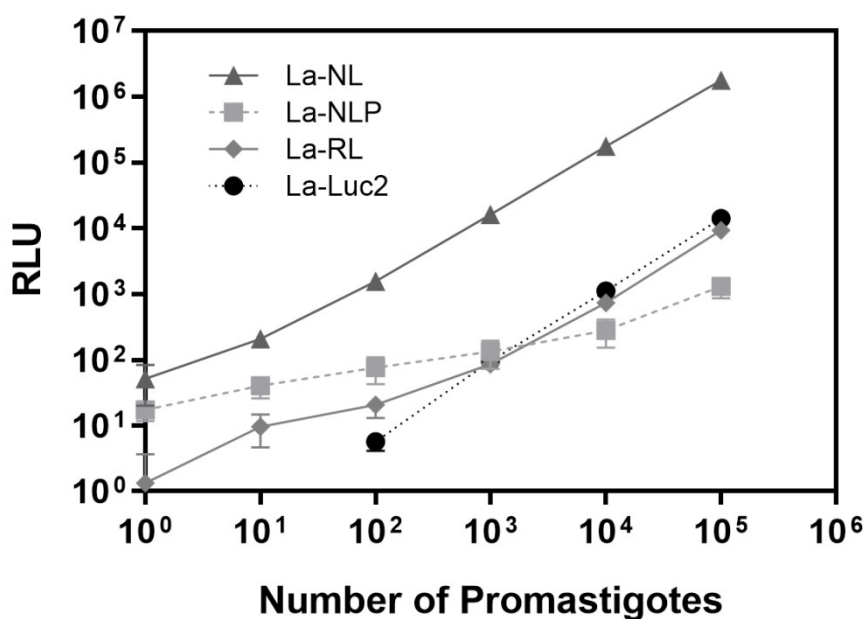
232 The infectivity *in vivo* of each mutant line was evaluated in the BALB/c mice model.
 233 Lesion development in mice infected with the mutant lines was delayed when compared to
 234 WT parasites (Supplementary Material Fig. S1). This reduced virulence could be related to
 235 the number of *in vitro* parasite sub-cultures (Magalhães et al., 2014); however, repeated
 236 infections in mice did not accelerate lesion development. Although the La-Luc2 line, previously
 237 obtained by the same method, maintained its infectivity profile, the possibility of impairment of
 238 the *in vivo* fitness of luciferase mutant parasites by the expression of those particular proteins
 239 cannot be excluded at present. Other studies in *L. infantum* expressing red-shifted luciferases
 240 have been done and did not report infectivity changes (Álvarez-Velilla et al., 2019; Eberhardt
 241 et al., 2019).

242

243 **2.2. Bioluminescence of promastigotes expressing NL, NLP and RL**

244 Luciferase activity of mutant lines was evaluated by analysing light production of
 245 serially diluted promastigotes incubated in the presence of their respective substrates (Fig.
 246 2A). Promastigotes expressing the conventional luciferase Luc2 (Trinconi et al., 2018) were
 247 also evaluated and used as a reference. Light emission, expressed in relative
 248 bioluminescence units (RLU), was linearly correlated with the number of parasites ($r^2 >$
 249 0.9894). NL-expressing parasites were the brightest with light output up to 1000-fold higher
 250 than NLP and over 100-fold higher than RL and Luc2 (Fig. 2). NLP produced the narrowest
 251 range of light intensity output throughout the curve. The sensitivity for detecting RL-expressing
 252 parasites was higher than Luc2 when 100 or less parasites were assayed. The curve profiles
 253 for RL and Luc2 promastigotes overlapped when more than 1000 parasites were evaluated.
 254 The detection limits for light production by NL, NLP and RL were 1, 10 and 10 parasites,
 255 respectively, while 100 parasites were necessary to detect Luc2 bioluminescence.

256 Light output from these parasites increased over the course of 60 minutes after
 257 substrate addition, but maintained the bioluminescence curve profiles (Supplementary
 258 Material Fig. S2).



259

260 **Figure 2. Luciferase activity in promastigotes of *L. amazonensis* transfected lines.**
261 Promastigotes were serially diluted and bioluminescence was measured 10 minutes after
262 substrate addition. Results are the mean and standard deviation of a representative
263 experiment of three independent experiments. RLU: relative light units.

264

265 La-NL and La-NLP light emission patterns were in agreement with findings described
266 by Hall et al. (2012), who developed NL and its derivatives through enzyme optimization and
267 coelenterazine modification. An intracellular half-life of at least 6 hours for the NL protein, as
268 opposed to 3 hours for Luc2 (Thorne et al., 2010), leads to NL accumulation in eukaryotic cells
269 and, in theory, to a greater light production. In fact, NL half-life in *L. mexicana* mutant lines
270 was demonstrated to be greater than 8 hours (Berry et al., 2018). Therefore, NL demonstrated
271 better *in vitro* performance in comparison to all the other luciferases tested with a light
272 emission 100 to 1000 times more intense, including the conventional luciferase, Luc2.

273 On the other hand, NL slow kinetics of decay made it too stable to be used in
274 promastigote viability assays, which was also seen in NL-expressing *L. mexicana* parasites
275 (Berry et al., 2018). For example, in conventional 24-hour assays using increasing
276 concentrations of amphotericin B against promastigotes expressing NL, it was not possible to
277 detect the expected decline in light intensity in treated parasites (Supplementary Material
278 Figure S3). For that reason, further *in vitro* experiments were performed using NLP, RL and
279 Luc2, whereas NL was saved for *in vivo* testing.

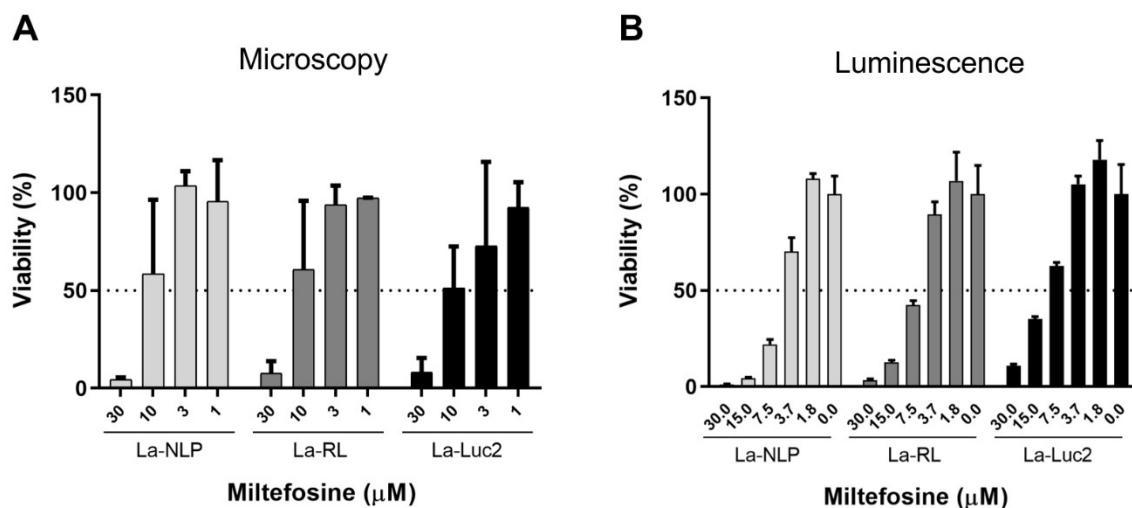
280

281 **2.3. Drug susceptibility testing in intracellular amastigotes**

282 To test these mutant lines in drug susceptibility assays, macrophages infected with La-
283 NLP, La-RL and La-Luc2 were treated with different concentrations of miltefosine (Fig. 3 and
284 Table 2) and the percentage of infected macrophages was determined after 72h by standard
285 microscopy or bioluminescence intensity. Miltefosine was chosen given its good activity
286 against *L. amazonensis* *in vitro* and *in vivo* (Coelho et al., 2014). The calculated IC₅₀ values
287 were statistically similar between the mutants for both methods (Table 2). The
288 bioluminescence assay produced robust dose-response curves, consistent in all mutants. All
289 three luciferases – NLP, RL and Luc2 – showed to be equally effective in the assessment of

290 drug susceptibility in intracellular amastigotes (Fig. 3B). The results determined through
 291 optical microscopy revealed wider standard deviations and therefore higher variability (Fig.
 292 3A). This can be explained by the method's limitations, such as the examiner's choice of fields
 293 to count.

294



295

296 **Figure 3. Comparison of bioluminescence and microscopy for the evaluation of drug**
 297 **susceptibility.** Macrophages infected with La-NLP, La-RL and La-Luc2 were treated with
 298 increasing concentrations of miltefosine for 72 hours. Parasite viability was determined using
 299 microscopy **(A)** and bioluminescence-based **(B)** techniques. Viability was calculated in
 300 reference to the untreated control, considered as 100% viable, for each line. Data are mean
 301 and standard deviation of at least three independent experiments.

302

303 Table 2. Miltefosine IC₅₀ for intracellular amastigotes calculated by bioluminescence or
 304 microscopy.

Lines	Bioluminescence ^a	Microscopy ^a
La-NLP	6.96 ± 0.99	11.85 ± 3.32
La-RL	7.67 ± 1.46	12.4 ± 3.36
La-Luc2	7.71 ± 1.71	8.32 ± 3.43

305

306 ^a Results are the average and standard error of the mean (SEM) of at least three

307 independent experiments.

308

309 We showed that NLP, RL and Luc2 were equally able to report amastigote viability.
310 Interestingly, light intensity from La-NLP and La-RL in intracellular amastigotes were higher
311 than light emitted by La-Luc2 (Supplementary Material Figure S4) while the opposite was
312 observed for promastigotes (Fig. 2, Supp. Fig. S2). A distinct rate of NLP/RL protein or RNA
313 degradation in amastigotes might explain this observation. The cassettes with NLP and RL
314 genes contain the *L. mexicana* cysteine protease B 2.8 3' untranslated region (UTR),
315 downstream to the NLP or RL genes. On the other hand, the Luc2 cassette has the tubulin 3'
316 UTR downstream to the coding sequence. The CPB UTR, originally derived from a stage-
317 regulated gene, may be driving this increased bioluminescence in amastigotes (Mißlitz et al.,
318 2000; Brooks et al., 2001).

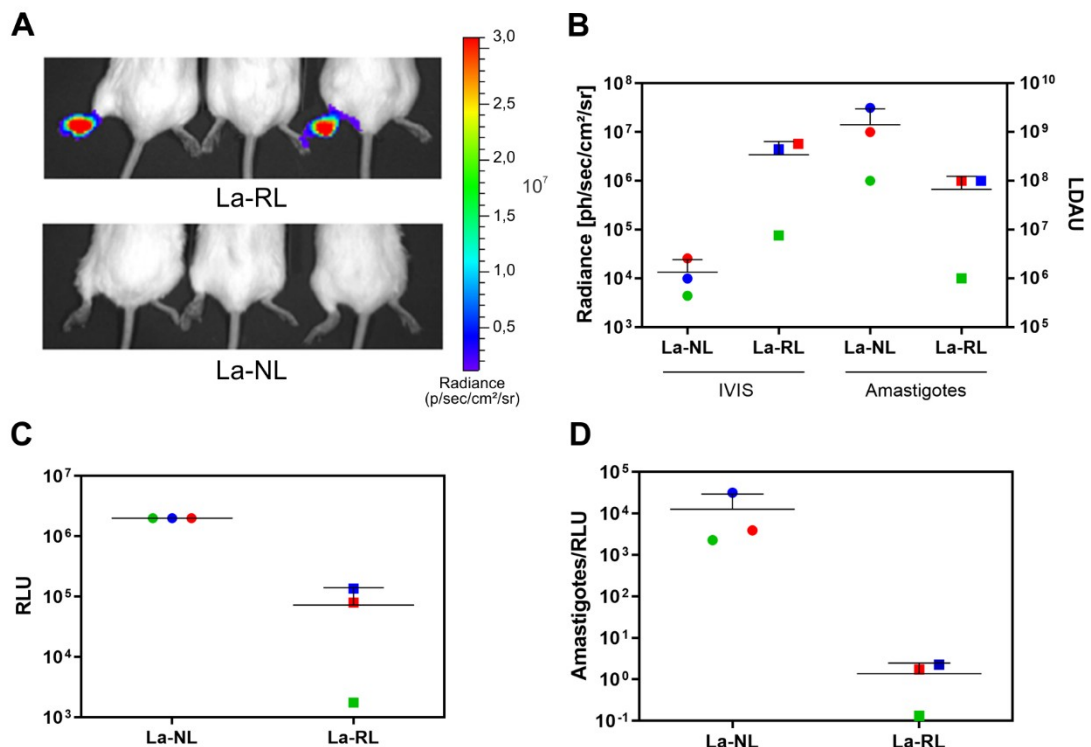
319

320 **2.4. Comparison of modified luciferases in an *in vivo* model**

321 In order to compare the *in vivo* bioluminescence of the modified luciferases, mutant
322 lines with higher *in vitro* light emission - La-NL and La-RL - were selected. BALB/c mice were
323 infected with La-NL and La-RL and parasite load was evaluated by bioimaging and limiting
324 dilution once lesions were well established. Parasite burden determined by limiting dilution
325 was at least 10-fold higher in La-NL-infected animals than in La-RL-infected mice (Figure 4B).
326 Conversely, bioluminescence detected from La-RL infected animals was up to 1000-fold
327 greater than light from La-NL mice (Figure 4A and 4B). Amastigotes freshly extracted from
328 lesions were also used to determine *ex vivo* bioluminescence and qualitatively compare the
329 parasite burden between infected animals (Figure 4C). *In vitro* light emission in the La-NL
330 lesion extracts was higher than in La-RL lesions, confirming the higher parasite burden of La-
331 NL-infected mice detected by limiting dilution. The ratio between the number of amastigotes
332 detected in the limiting dilution assay by the relative light units detected by bioimaging was
333 used as an arbitrary measure of *in vivo* sensitivity (Fig. 4D). The putative number of
334 amastigotes necessary to emit one RLU *in vivo* was 1000-fold greater for La-NL than La-RL.

335 Light produced by the reaction of RL and its substrate is emitted within a narrow
336 spectrum above 600 nm, as shown by studies with similar luciferases (Branchini et al., 2005b;

2010). NL, on the other hand, produces a narrow spectrum at 450 nm. Results shown here are consistent with the previous understanding that La-RL derived light may overcome tissue barriers more efficiently than light produced by La-NL. Our experiments showed that animals infected with La-RL that developed lesions with approximately 10^6 parasites displayed greater levels of bioluminescence than La-NL lesions bearing about 10^9 amastigotes.



343

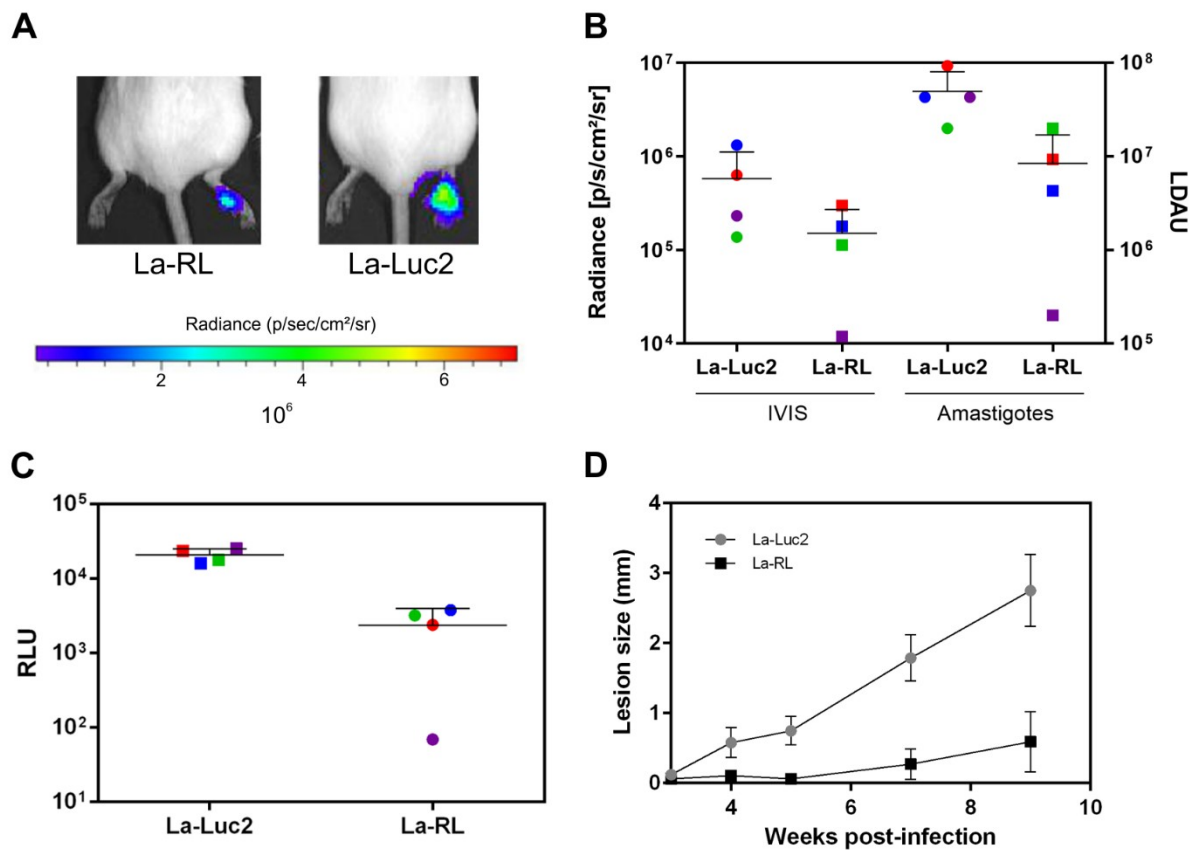
Figure 4. Comparison of *in vivo* and *ex vivo* bioluminescence emission by La-NL and La-RL-infected mice. BALB/c mice (n = 3) were inoculated with 10^6 La-NL or La-RL promastigotes at the left hind footpad. The parasite burden was evaluated at the 31st week post infection by *in vivo* bioluminescence imaging (A and B), limiting dilution (B) and *ex vivo* bioluminescence (C). The putative number of amastigotes per RLU captured during bioimaging was calculated as the ratio between amastigotes detected by limiting dilution and relative light units (D). IVIS: *in vivo* imaging system; LDAU: limiting dilution assay units, meaning total number of amastigotes in the footpad; RLU: relative light units.

352

353 Considering the *in vivo* performance of La-RL, the mutant line was moved forward to be compared with Luc2, the conventional firefly luciferase. La-RL or La-Luc2 infected mice were evaluated nine weeks post infection by bioimaging and limiting dilution (Fig. 5A and B). A slower progression in lesion size was observed in the group infected with La-RL (Fig. 5D). In agreement with that observation, the parasite burden was about 6-fold higher in La-Luc2

357

358 infections compared with La-RL-infected mice (Fig. 5B). A bioluminescence pattern congruent
 359 with the limiting dilution data was observed (Fig. 5A and B). The *ex vivo* amastigote
 360 bioluminescence assay confirmed the difference in parasite burden between groups with a
 361 more uniform signal within the group (Fig. 5C) compared to bioimaging and limiting dilution
 362 quantifications. The *in vivo* light output was not statistically different between groups.
 363



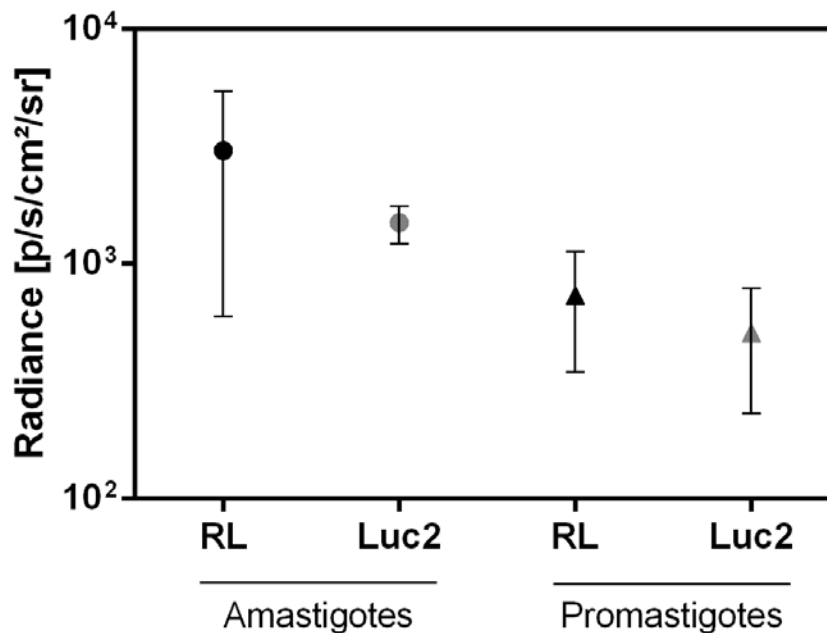
364

365 **Figure 5. *In vivo* and *ex vivo* comparison of light emission between La-RL and La-Luc2.**
 366 BALB/c mice (n = 4) were inoculated with 10⁶ La-RL or La-Luc2 promastigotes at the left hind
 367 footpad. Parasite burden was determined after 9 weeks of infection by bioimaging (A and B),
 368 limiting dilution (B) and *ex vivo* bioluminescence activity of amastigotes (C). Colours represent
 369 the same animal over different experiments. (D) Follow up of the lesion size. Data are the
 370 average and standard deviation of the biological replicates.
 371

372 Aiming to avoid the influence of any differences in lesion development between the La-
 373 RL and La-Luc2 lines, mice were bioimaged 1 hour after inoculation with a fixed number of
 374 parasites. Freshly purified lesion-derived amastigotes or stationary phase-promastigotes were
 375 injected at the anterior and posterior footpads. One hour later, bioluminescence was

376 measured. No significant differences were observed between footpads inoculated with
 377 amastigotes and promastigotes of the same line. The comparison of light intensity emitted by
 378 La-RL and La-Luc2 was also statistically identical, indicating equivalent *in vivo* detection for
 379 RL and Luc2 as reporters in a cutaneous leishmaniasis model.

380



381

382 **Figure 6. *In vivo* bioluminescence of 10⁵ promastigotes or amastigotes of La-RL and**
 383 **La-Luc2.** BALB/c mice (n = 2) were inoculated in the footpad with 10⁵ promastigotes or
 384 amastigotes. Bioluminescence was evaluated 1-hour post-inoculation. Data are the average and standard deviation of the biological replicates. RLU: relative light units.

385

386

387 RL showed to be a promising viability reporter both in *in vitro* and *in vivo* assays.
 388 Unexpectedly, RL displayed sensitivity similar to Luc2 in our model, even though its light is
 389 emitted in a wavelength above 600 nm. According to Liang et al. (2012), Luc2 produces light
 390 in a broad spectrum of emission, from 540 to 640 nm. Although some of this light may be
 391 blocked by tissues, as with NL, part of it is emitted over 600 nm and therefore interference
 392 would be less important. On the other hand, in a model where skin lesions are being evaluated,
 393 less tissue barriers are present. Nevertheless, there is still room to investigate the use of this
 394 luciferase in visceral leishmaniasis, where the light emitted by the parasite might encounter

395 more tissue barriers. Our findings lead to the conclusion that, as observed for Luc2, RL was
396 effective for both *in vitro* and *in vivo* viability assays while NLP is a good option for *in vitro*
397 studies.

398 New strategies for imaging will bring great benefits onto biological preclinical
399 evaluation of drugs and diseases. Interesting avenues are being pursued by improving
400 reporter enzymes as well as the bioluminescence properties of the substrates (Kuchimaru et
401 al., 2016; Iwano et al., 2018), or both (Yeh et al., 2017). For example, a near infrared shift on
402 emission obtained by a modified luciferase substrate resulted in great improvements in
403 sensitivity of detection particularly from deep tissues (Kuchimaru et al., 2016) and even
404 allowing detection of single cells in deep tissues of live animals (Iwano et al., 2018). These
405 tools are beginning to be employed to study the relationship between parasites and their hosts
406 and are opening a whole new set of possibilities (De Niz et al., 2019).

407

408 **4. Conclusion**

409 Altogether, these findings bring new insights regarding the use of modified luciferases
410 in the drug discovery process for infectious diseases. NL demonstrated strong *in vitro*
411 bioluminescence and higher stability over the other luciferases. However, its application might
412 be somewhat restricted to *in vitro* experiments here unexplored, whereas Luc2 and RL have
413 apparently greater *in vivo* application, even though their light emission *in vitro* is less intense
414 than NL. All luciferases, except for NL, showed to be useful tools in the report of intracellular
415 amastigotes viability. Finally, we have demonstrated that a red-shifted luciferase does not
416 enhance light detection in a cutaneous leishmaniasis model, displaying similar *in vivo*
417 bioluminescent potential in comparison to the conventional luciferase, Luc2.

418

419 **Acknowledgements**

420 We would like to thank Caroline R. Espada, Jenicer K. U. Yokoyama-Yasunaka and Marinete
421 Pedro da Silva for all the support, technical assistance and constructive discussions.

422

423 Funding

424 This work was supported by the Fundação de Amparo à Pesquisa do Estado de São Paulo
425 [grant number 2015/09080-2], Brazil. This study was financed in part by the Coordenação de
426 Aperfeiçoamento de Pessoal de Nível Superior - Brasil (CAPES) - Finance Code 001. SRBU
427 is the recipient of a senior researcher scholarship from CNPq. VSA and CT were fellows
428 supported by FAPESP (2015/26121-4 and 2015/23832-7, respectively).

429 **References**

- 430 Akhoundi, M., Kuhls, K., Cannet, A., Votýpka, J., Marty, P., Delaunay, P., Sereno, D., 2016.
431 A Historical overview of the classification, evolution, and dispersion of *Leishmania*
432 parasites and sandflies. PLoS Negl. Trop. Dis. 10, 1–40.
433 <https://doi.org/10.1371/journal.pntd.0004349>
- 434 Álvarez-Velilla, R., Gutiérrez-Corbo, M. del C., Punzón, C., Pérez-Pertejo, M.Y., Balaña-
435 Fouce, R., Fresno, M., Reguera, R.M., 2019. A chronic bioluminescent model of
436 experimental visceral leishmaniasis for accelerating drug discovery. PLoS Negl. Trop.
437 Dis. 13, 1–15. <https://doi.org/10.1371/journal.pntd.0007133>
- 438 Avci, P., Karimi, M., Sadasivam, M., Antunes-Melo, W.C., Carrasco, E., Hamblin, M.R.,
439 2018. In-vivo monitoring of infectious diseases in living animals using bioluminescence
440 imaging. Virulence 9, 28–63. <https://doi.org/10.1080/21505594.2017.1371897>
- 441 Bern, C., Desjeux, P., Cano, J., Alvar, J., 2012. Leishmaniasis Worldwide and Global
442 Estimates of Its Incidence 7. <https://doi.org/10.1371/journal.pone.0035671>
- 443 Berry, S.L., Hameed, H., Thomason, A., Maciej-Hulme, M.L., Saif Abou-Akkada, S.,
444 Horrocks, P., Price, H.P., 2018. Development of NanoLuc-PEST expressing
445 *Leishmania mexicana* as a new drug discovery tool for axenic- and intramacrophage-
446 based assays. PLoS Negl. Trop. Dis. 12, 1–20.
447 <https://doi.org/10.1371/journal.pntd.0006639>
- 448 Branchini, B.R., Ablamsky, D.M., Davis, A.L., Southworth, T.L., Butler, B., Fan, F., Jathoul,
449 A.P., Pule, M.A., 2010. Red-emitting luciferases for bioluminescence reporter and
450 imaging applications. Anal. Biochem. 396, 290–297.
451 <https://doi.org/10.1016/j.ab.2009.09.009>
- 452 Branchini, Bruce R., Southworth, T.L., Khattak, N.F., Michelini, E., Roda, A., 2005. Red- and
453 green-emitting firefly luciferase mutants for bioluminescent reporter applications. Anal.
454 Biochem. 345, 140–148. <https://doi.org/10.1016/j.ab.2005.07.015>
- 455 Branchini, Bruce R., Southworth, T.L., Murtiashaw, M.H., Wilkinson, S.R., Khattak, N.F.,
456 Rosenberg, J.C., Zimmer, M., 2005. Mutagenesis evidence that the partial reactions of

- 457 firefly bioluminescence are catalyzed by different conformations of the luciferase C-
458 terminal domain. *Biochemistry* 44, 1385–93. <https://doi.org/10.1021/bi047903f>
- 459 Brooks, D.R., Denise, H., Westrop, G.D., Coombs, G.H., Mottram, J.C., 2001. The Stage-
460 regulated expression of *Leishmania mexicana* CPB cysteine proteases is mediated by
461 an intercistronic sequence element. *J. Biol. Chem.* 276, 47061–47069.
462 <https://doi.org/10.1074/jbc.M108498200>
- 463 Burza, S., Croft, S.L., Boelaert, M., 2018. Leishmaniasis. *Lancet*.
464 [https://doi.org/10.1016/S0140-6736\(18\)31204-2](https://doi.org/10.1016/S0140-6736(18)31204-2)
- 465 Calvo-Alvarez, E., Cren-Travaillé, C., Cruzols, A., Rotureau, B., 2018. A new chimeric triple
466 reporter fusion protein as a tool for *in vitro* and *in vivo* multimodal imaging to monitor
467 the development of African trypanosomes and *Leishmania* parasites. *Infect. Genet.*
468 *Evol.* <https://doi.org/10.1016/j.meegid.2018.01.011>
- 469 Calvo-Álvarez, E., Stamatakis, K., Punzón, C., Álvarez-Velilla, R., Tejería, A., Escudero-
470 Martínez, J.M., Pérez-Pertejo, Y., Fresno, M., Balaña-Fouce, R., Reguera, R.M., 2015.
471 Infrared Fluorescent Imaging as a Potent Tool for *In Vitro*, *Ex Vivo* and *In Vivo* Models
472 of Visceral Leishmaniasis. *PLoS Negl. Trop. Dis.* 9, 1–19.
473 <https://doi.org/10.1371/journal.pntd.0003666>
- 474 Coburn, C.M., Otteman, K.M., McNeely, T., Turco, S.J., Beverley, S.M., 1991. Stable DNA
475 transfection of a wide range of trypanosomatids. *Mol. Biochem. Parasitol.* 46, 169–79.
476 [https://doi.org/10.1016/0166-6851\(91\)90210-W](https://doi.org/10.1016/0166-6851(91)90210-W)
- 477 Coelho, A.C., Trinconi, C.T., Costa, C.H.N., Uliana, S.R.B., 2014. *In Vitro* and *In Vivo*
478 Miltefosine Susceptibility of a *Leishmania amazonensis* Isolate from a Patient with
479 Diffuse Cutaneous Leishmaniasis. *PLoS Negl. Trop. Dis.* 8, 1–11.
480 <https://doi.org/10.1371/journal.pntd.0002999>
- 481 Convit, J., Fernandez, C., Tapia, F., Caceres-Dittmar, G., Castés, M., Rondon, A., Ulrich, M.,
482 1993. The clinical and immunological spectrum of American cutaneous leishmaniasis.
483 *Trans. R. Soc. Trop. Med. Hyg.* 87, 444–448.
- 484 De Niz, M., Spadin, F., Marti, M., Stein, J. V., Frenz, M., Frischknecht, F., 2019. Toolbox for

- 485 *In Vivo* Imaging of Host–Parasite Interactions at Multiple Scales. *Trends Parasitol.* 35,
486 193–212. <https://doi.org/10.1016/j.pt.2019.01.002>
- 487 Eberhardt, E., Bulté, D., Van Bockstal, L., Van Den Kerkhof, M., Cos, P., Delputte, P.,
488 Hendrickx, S., Maes, L., Caljon, G., 2019. Miltefosine enhances the fitness of a non-
489 virulent drug-resistant *Leishmania infantum* strain. *J. Antimicrob. Chemother.* 74, 395–
490 406. <https://doi.org/10.1093/jac/dky450>
- 491 García-Alai, M.M., Gallo, M., Salame, M., Wetzler, D.E., McBride, A.A., Paci, M., Cicero,
492 D.O., de Prat-Gay, G., 2006. Molecular Basis for Phosphorylation-Dependent, PEST-
493 Mediated Protein Turnover. *Structure* 14, 309–319.
494 <https://doi.org/10.1016/j.str.2005.11.012>
- 495 Hall, M.P., Unch, J., Binkowski, B.F., Valley, M.P., Butler, B.L., Wood, M.G., Otto, P.,
496 Zimmerman, K., Vidugiris, G., MacHleidt, T., Robers, M.B., Benink, H. a., Eggers, C.T.,
497 Slater, M.R., Meisenheimer, P.L., Klaubert, D.H., Fan, F., Encell, L.P., Wood, K. V.,
498 2012. Engineered luciferase reporter from a deep sea shrimp utilizing a novel
499 imidazopyrazinone substrate. *ACS Chem. Biol.* 7, 1848–1857.
500 <https://doi.org/10.1021/cb3002478>
- 501 Iwano, S., Sugiyama, M., Hama, H., Watakabe, A., Hasegawa, N., Kuchimaru, T., Tanaka,
502 K.Z., Takahashi, M., Ishida, Y., Hata, J., Shimosono, S., Namiki, K., Fukano, T.,
503 Kiyama, M., Okano, H., Kizaka-kondoh, S., Mchugh, T.J., Yamamori, T., Hioki, H.,
504 Maki, S., Miyawaki, A., 2018. Single-cell bioluminescence imaging of deep tissue in
505 freely moving animals. *Science* (80-). 939, 935–939.
- 506 Jaiswal, A.K., Rao, K.B., Kushwaha, P., Rawat, K., Modukuri, R.K., Khare, P., Joshi, S.,
507 Mishra, S., Rai, A., Sashidhara, K. V., Dube, A., 2016. Development of *Leishmania*
508 *donovani* stably expressing DsRed for flow cytometry-based drug screening using
509 chalcone thiazolyl-hydrazone as a new antileishmanial target. *Int. J. Antimicrob.*
510 *Agents.* <https://doi.org/10.1016/j.ijantimicag.2016.09.018>
- 511 Kuchimaru, T., Iwano, S., Kiyama, M., Mitsumata, S., Kadonosono, T., Niwa, H., Maki, S.,
512 Kizaka-Kondoh, S., 2016. A luciferin analogue generating near-infrared

- 513 bioluminescence achieves highly sensitive deep-tissue imaging. Nat. Commun. 7, 1–8.
514 <https://doi.org/10.1038/ncomms11856>
- 515 Lima, H.C., Bleyenbergh, J.A., Titus, R.G., 1997. A simple method for quantifying *Leishmania*
516 in tissues of infected animals. Parasitol. Today 13, 80–82.
517 [https://doi.org/10.1016/S0169-4758\(96\)40010-2](https://doi.org/10.1016/S0169-4758(96)40010-2)
- 518 Magalhães, R.D.M., Duarte, M.C., Mattos, E.C., Martins, V.T., Lage, P.S., Chávez-
519 Fumagalli, M.A., Lage, D.P., Menezes-Souza, D., Régis, W.C.B., Manso Alves, M.J.,
520 Soto, M., Tavares, C.A.P., Nagen, R.A.P., Coelho, E.A.F., 2014. Identification of
521 Differentially Expressed Proteins from *Leishmania amazonensis* Associated with the
522 Loss of Virulence of the Parasites. PLoS Negl. Trop. Dis. 8.
523 <https://doi.org/10.1371/journal.pntd.0002764>
- 524 Mißlitz, A., Mottram, J.C., Overath, P., Aebischer, T., 2000. Targeted integration into a rRNA
525 locus results in uniform and high level expression of transgenes in *Leishmania*
526 amastigotes. Mol. Biochem. Parasitol. 107, 251–261. [https://doi.org/10.1016/S0166-6851\(00\)00195-X](https://doi.org/10.1016/S0166-6851(00)00195-X)
- 528 Ponte-Sucre, A., Gamarro, F., Dujardin, J.-C., Barrett, M.P., López-Vélez, R., García-
529 Hernández, R., Pountain, A.W., Mwenechanya, R., Papadopoulou, B., 2017. Drug
530 resistance and treatment failure in leishmaniasis: A 21st century challenge. PLoS Negl.
531 Trop. Dis. 11, e0006052. <https://doi.org/10.1371/journal.pntd.0006052>
- 532 Rechsteiner, M., Rogers, S.W., 1996. PEST sequences and regulation by proteolysis.
533 Trends Biochem. Sci. 21, 267–271. [https://doi.org/10.1016/0968-0004\(96\)10031-1](https://doi.org/10.1016/0968-0004(96)10031-1)
- 534 Reimão, J.Q., Oliveira, J.C., Trinconi, C.T., Cotrim, P.C., Coelho, A.C., Uliana, S.R.B., 2015.
535 Generation of Luciferase-Expressing *Leishmania infantum chagasi* and Assessment of
536 Miltefosine Efficacy in Infected Hamsters through Bioimaging. PLoS Negl. Trop. Dis. 9,
537 e0003556. <https://doi.org/10.1371/journal.pntd.0003556>
- 538 Reimão, J.Q., Trinconi, C.T., Yokoyama-Yasunaka, J.K., Miguel, D.C., Kalil, S.P., Uliana,
539 S.R.B., 2013. Parasite burden in *Leishmania (Leishmania) amazonensis*-infected mice:
540 Validation of luciferase as a quantitative tool. J. Microbiol. Methods 93, 95–101.

- 541 <https://doi.org/10.1016/j.mimet.2013.02.007>
- 542 Rocha, M.N., Corrêa, C.M., Melo, M.N., Beverley, S.M., Martins-Filho, O.A., Madureira, A.P.,
543 Soares, R.P., 2013. An alternative *in vitro* drug screening test using *Leishmania*
544 *amazonensis* transfected with red fluorescent protein. *Diagn. Microbiol. Infect. Dis.*
545 <https://doi.org/10.1016/j.diagmicrobio.2012.11.018>
- 546 Sundar, S., Olliaro, P.L., 2007. Miltefosine in the treatment of leishmaniasis: Clinical
547 evidence for informed clinical risk management. *Ther. Clin. Risk Manag.* 3, 733–40.
- 548 Sundar, S., Singh, A., 2018. Chemotherapeutics of Visceral Leishmaniasis: present and
549 future developments. *Parasitology* 145, 481–489.
550 <https://doi.org/10.1016/j.physbeh.2017.03.040>
- 551 Thorne, N., Inglese, J., Auld, D.S., 2010. Illuminating Insights into Firefly Luciferase and
552 Other Bioluminescent Reporters Used in Chemical Biology. *Chem. Biol.* 17, 646–657.
553 <https://doi.org/10.1016/j.chembiol.2010.05.012>
- 554 Trinconi, C.T., Reimão, J.Q., Bonano, V.I., Espada, C.R., Miguel, D.C., Yokoyama-
555 Yasunaka, J.K.U., Uliana, S.R.B., 2018. Topical tamoxifen in the therapy of cutaneous
556 leishmaniasis. *Parasitology* 1–7. <https://doi.org/10.1017/S0031182017000130>
- 557 Trinconi, C.T., Reimão, J.Q., Coelho, A.C., Uliana, S.R.B., 2016. Efficacy of tamoxifen and
558 miltefosine combined therapy for cutaneous leishmaniasis in the murine model of
559 infection with *Leishmania amazonensis*. *J. Antimicrob. Chemother.* 71, 1314–1322.
560 <https://doi.org/10.1093/jac/dkv495>
- 561 Uliana, S.R.B., Affonso, M.H.T., Camargo, E.P., Floeter-Winter, L.M., 1991. *Leishmania*:
562 Genus identification based on a specific sequence of the 18S ribosomal RNA
563 sequence. *Exp. Parasitol.* 72, 157–163. [https://doi.org/10.1016/0014-4894\(91\)90133-H](https://doi.org/10.1016/0014-4894(91)90133-H)
- 564 Uliana, S.R.B., Goyal, N., Freymüller, E., Smith, D.F., 1999. *Leishmania*: Overexpression
565 and comparative structural analysis of the stage-regulated meta 1 gene. *Exp. Parasitol.*
566 92, 183–191. <https://doi.org/10.1006/expr.1999.4410>
- 567 Uliana, S.R.B., Trinconi, C.T., Coelho, A.C., 2017. Chemotherapy of leishmaniasis: present
568 challenges. *Parasitology* 1–17. <https://doi.org/10.1017/S0031182016002523>

- 569 Yan, Y., Shi, P., Song, W., Bi, S., 2019. Chemiluminescence and bioluminescence imaging
570 for biosensing and therapy: *In vitro* and *in vivo* perspectives. *Theranostics* 9, 4047–
571 4065. <https://doi.org/10.7150/thno.33228>
- 572 Yeh, H.-W., Karmach, O., Ji, A., Carter, D., Martins-Green, M.M., Ai, H., 2017. Red-shifted
573 luciferase–luciferin pairs for enhanced bioluminescence imaging. *Nat. Methods* 14,
574 971–974. <https://doi.org/10.1038/nmeth.4400>
- 575 Zerpa, O., Ulrich, M., Blanco, B., Polegre, M., Avila, A., Matos, N., Mendoza, I., Pratlong, F.,
576 Ravel, C., Convit, J., 2007. Diffuse cutaneous leishmaniasis responds to miltefosine but
577 then relapses. *Br. J. Dermatol.* 156, 1328–1335. [https://doi.org/10.1111/j.1365-](https://doi.org/10.1111/j.1365-2133.2007.07872.x)
578 [2133.2007.07872.x](https://doi.org/10.1111/j.1365-2133.2007.07872.x)
- 579

Manuscript

Evaluation of NanoLuc, RedLuc and Luc2 as bioluminescent reporters in a cutaneous leishmaniasis model by Agostino et al.

Declaration of interests

The authors declare that they have no known competing financial interests or personal relationships that could have appeared to influence the work reported in this paper.

The authors declare the following financial interests/personal relationships which may be considered as potential competing interests:

Supplementary Material

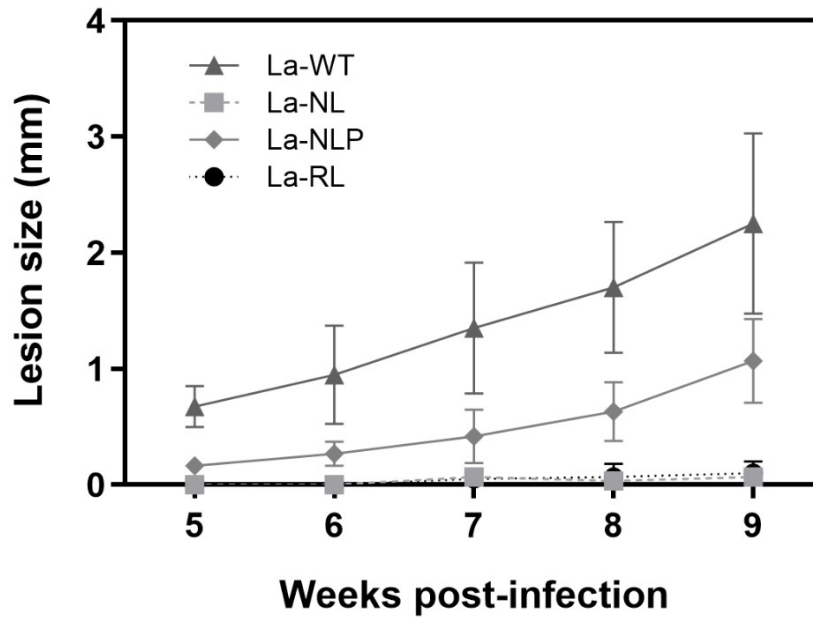


Figure S1. Lesion development in BALB/c mice infected with *L. amazonensis* WT and mutants expressing NL, NLP and RL. Animals (n = 3) were infected with 3×10^6 stationary-phase promastigotes and lesion development was monitored weekly from the 5th week post-infection with a caliper. Data represents the difference between the size of infected and contralateral healthy footpad.

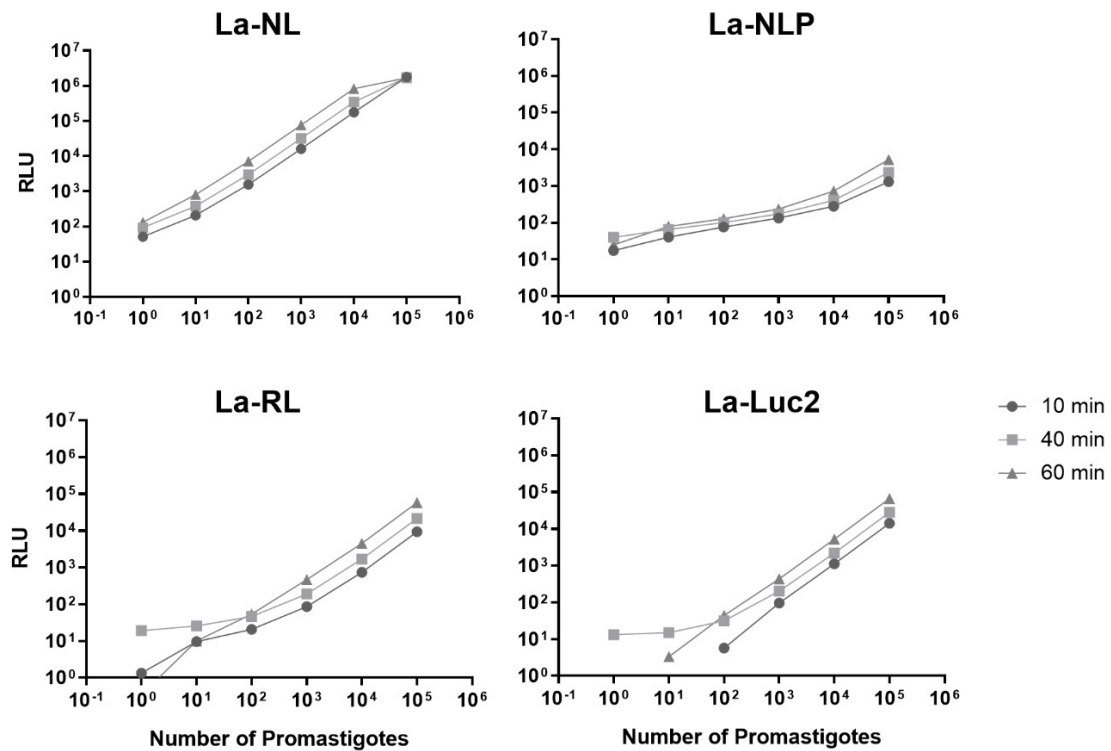


Figure S2. Luminescence of *L. amazonensis* promastigotes expressing NL, NLP, RL and Luc2. Promastigotes were serially diluted (logarithmic base) and luminescence was measured using a microplate reader 10, 40 and 60 minutes after substrate addition. Results are the mean and standard deviation of a representative experiment of three independent experiments. RLU: relative light units.

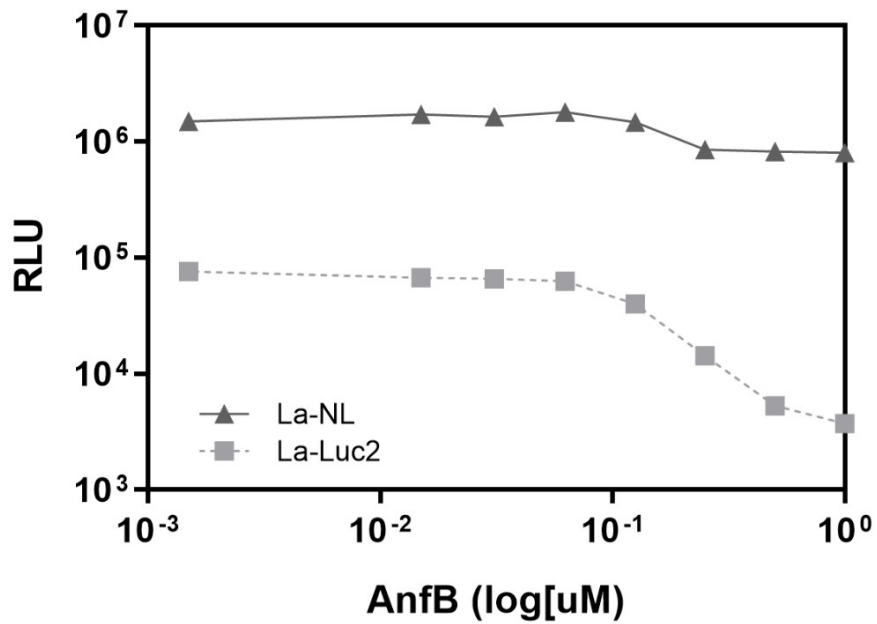


Figure S3. Susceptibility of La-NL and La-Luc2 lines to amphotericin B determined by luminescence. Promastigotes were treated in triplicates with increasing concentrations of amphotericin B for 24 hours in white 96-well plates. Adequate substrates were added, and luminescence was obtained after 10 minutes. Data represents the mean and standard deviation of a representative experiment of three independent experiments.

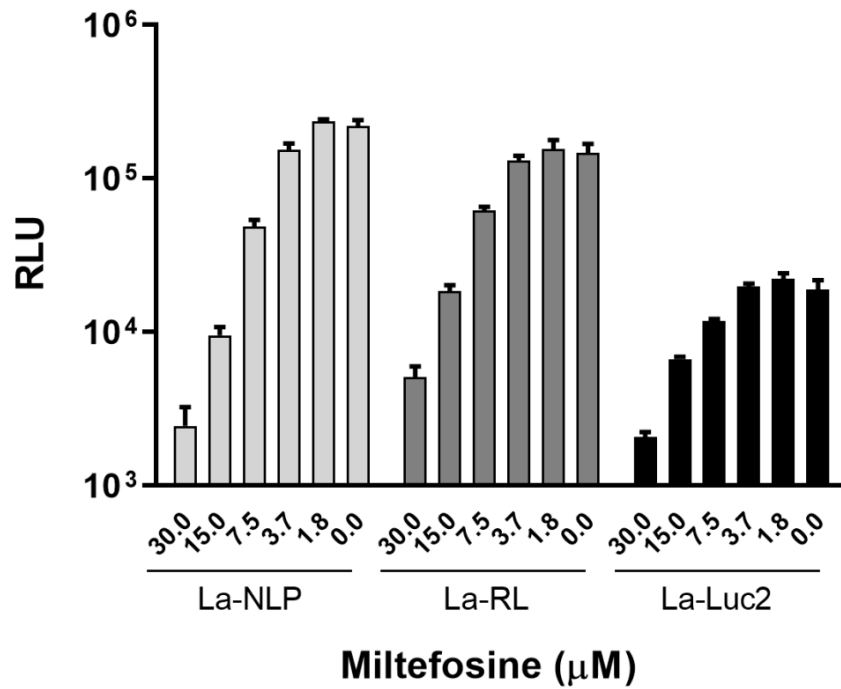


Figure S4. Susceptibility of La-NLP, La_{RL} and La-Luc2 intramacrophage amastigotes determined by luminescence. Macrophages infected with La-NLP, La-RL and La-Luc2 were treated with increasing concentrations of miltefosine for 72 hours. Data are mean and standard deviation of a representative experiment of three independent experiments.